JOURNAL OF SOLID STATE CHEMISTRY **135,** 175–181 (1998)
ARTICLE NO. SC977594

# On the Phase Transitions of $Bi_2Te_4O_{11}$

Gy. A. Lovas,* I. Dódony,* L. Pöppl,†,[1] and Zs. Szaller‡

*Mineralogical Department, L. Eötvös University, Múzeum krt. 4a, 1088 Budapest, Hungary; †Institute of Inorganic and Analytical Chemistry, L. Eötvös University, 112 Pf.32, 1518 Budapest, Hungary; and ‡Research Laboratory for Crystal Physics, Hungarian Academy of Sciences, Pf. 132, 1502 Budapest, Hungary

Received April 28, 1997; accepted August 18, 1997

**The polymorphic phase transitions of $Bi_2Te_4O_{11}$ have been investigated using X-ray powder diffraction (XPD), selected area electron diffraction (SAED), and differential scanning calorimetry (DSC) in the 25–730°C range. The metastable cubic modification, which forms under fast crystalization of the $Bi_2Te_4O_{11}$ melt, has fluorite-type structure. Each cation position is filled with bismuth and tellurium in 1/3–2/3 ratio, while the anion positions are occupied by oxygen in 11/12 site occupancy (evenly distributed vacancy), representing a structure with no chemical ordering. The first process in the transition of cubic phase is cation ordering along a cubic [111] direction. The ordering process has a small activation energy, but the structure reordering itself is exotherm. The final stage of this ordering is the separation of the cations into the triplets of planes forming two types of structural slabs with composition $Bi_2Te_2O_7$ and $TeO_2$. Every third plane contains only Te, and the first two are occupied by equal amounts, of Bi and Te with random distribution. The oxygen content is lower than what would be expected based on the available anion sites in the ideal fluorite structure, and these positions are populated by oxygen in a statistical (random) distribution. The next step of transition is the ordering of oxygen vacancy. The oxygen vacancy is concentrated at the Bi-containing layers in accordance with the fluorite-based structural model of the $Bi_2Te_2O_7$ layers. The result is monoclinic $Bi_2Te_4O_{11}$ with $P2_1/n$ symmetry. There are, however, several grains in the sample that show the coexistence of an exclusively cation-ordered, fluorite-type structure and that of Rossel's model. This indicates an intermediate or alternative stage of the phase transition, in which the $Bi_2Te_2O_7$ and $TeO_2$ slabs are already formed, but the oxygen coordination in the $TeO_2$ layer is still fluorite-type hexahedral. The formation of the rutile-type $TeO_2$ slabs can be a next step of the transition. The boundary between the two observed phases is irregular. The solid state first order phase transformation can be assumed at the grain boundaries.** © 1998 Academic Press

## INTRODUCTION

In a previous publication, L. Pöppl and co-workers have reported on phases of $Bi_2Te_4O_{11}$ found during the preparation by solid state reaction of $Bi_2O_3$ and $TeO_2$ in a 1:4 mol mixture (1). The SAED patterns proved the existence of the $Bi_2Te_4O_{11}$ in a fluorite structure with no chemical ordering. The cubic modification was formed by fast crystalization of the $Bi_2Te_4O_{11}$ melt. The main product of a slow cooling was the same cubic polymorph, though a subordinate formation of a monoclinic phase characterized by a superstructure of fluorite and rutile slabs, was also observed (2). The $\beta$-$Bi_2Te_4O_{11}$ cubic phase underwent a monotropic transformation into the $\alpha$-$Bi_2Te_4O_{11}$ monoclinic modification at temperatures higher than 400°C. The cubic → monoclinic transition has been interpreted as the result of an ordering in one set of $\{111\}$ planes and the change from orthogonality of the cubic phase in the [110] projection to monoclinic symmetry. The goal of the present study is to clarify the structural details of the transition between the cubic phase and the above monoclinic modification.

## EXPERIMENTAL

Starting materials were $Bi_2O_3$ (Johnson Matthey grade 1) and $TeO_2$ prepared from tellurium metal (99.999%) by oxidation with $HNO_3$ (Carlo Erba for analysis). After a short anneal in air at 450°C, the oxides were ground and sieved. The fraction with a grain size smaller than 63 μm was used for the synthesis.

The $Bi_2Te_4O_{11}$ sample was prepared from the mixture of $Bi_2O_3 + 4TeO_2$. The mixture was put into a platinum crucible, heated to 720°C in a furnace under argon atmosphere, held for 30 min at this temperature, and cooled by 10°C/min.

Three samples were subject to detailed structural analysis: sample A, which was formed from the solidification of the reaction melt; sample B, formed by annealing sample A at 520°C, and sample C, the annealation product at 620°C. The DSC measurements were carried out by a PL Thermal

[1] To whom all correspondence should be addressed.



0022-4596/98 $25.00

Sciences 1500 Differential Scanning Calorimeter (DSC) in flowing argon atmosphere (10 $cm^3$/min), using 10°C/min heating and cooling rates.

X-ray powder diffraction experiments were carried out using Cu$K\alpha$-radiation ($\lambda = 0.154178$ nm) on a Siemens D5000 powder diffractometer system with theta–theta Bragg-Brentano geometry, fixed slits, and a pyrolitic graphite secondary monochromator. The measurement control and all subsequent calculations were performed on the integrated computing facilities of the D5000 system. The intensity data were collected by the step-scan technique in the ranges 7.00–145.00° 2Θ (for sample A) and 7.00–103.00° 2Θ (for samples B and C), with a step width of 0.02° 2Θ. The Rietveld analysis was performed by means of the DBWS-9411 (3) program package; the graphical representation of the results was realized by DMPLOT (4).

Electron transparent samples were prepared by suspension technique. Pieces of the samples were crushed under ethanol, and drops of the suspension were allowed to dry on holey-carbon TEM grids. TEM images and SAED patterns were obtained at 200 kV with a Philips CM20 electron microscope equipped with a double-tilt GATAN goniometer stage. The electron micrographs of oriented crystals were recorded at optimum contrast using an objective aperture with radius 3.4 $Å^{-1}$ in the diffraction plane. The processing of digitized micrographs was performed on a Macintosh computer using Adobe Photoshop 3.0. The SAED pattern simulations and related calculations were done using MSI Cerius$^2$ software on an SGI workstation.

## RESULTS AND DISCUSSION

### *Investigation by DSC*

The DSC thermogram of $\beta$-$Bi_2Te_4O_{11}$ cubic phase can be seen in Fig. 1. A small and broad endothermic process takes place at 365.0°C onset temperature, upon which an exothermic process is superimposed ($T_{onset} = 438.4$°C). The latter was identified as the process belonging to the cubic-monoclinic phase transformation (1). A second sharp endothermic peak can be detected at 573.3°C onset temperature, before the melting point. Applying a heating and cooling cycles temperature program, it can be proved that the cubic-monoclinic transition is irreversible and that the second endothermic peak tends to disappear (Fig. 2). If the heating program is stopped after the first cycle and the temperature held at 600°C for one hour, the same result is obtained. On the basis of DSC results, two kinds of monoclinic phases can be assumed.

### *X-ray Powder Study*

First, sample A was investigated to verify that the cubic phase solidifying first from the reaction melt actually has the suggested *Fm*3*m* fluorite-type structure (1). The refinement results in Table 1 and Fig. 3 show that the starting point of the polymorphic phase transition of $Bi_2Te_4O_{11}$ is indeed the metastable cubic modification, as previously only hypothesized. Each cation position of the structure is filled with bismuth and tellurium in 1/3–2/3 ratio, while the anion positions are occupied by oxygen in 11/12 site occupancy

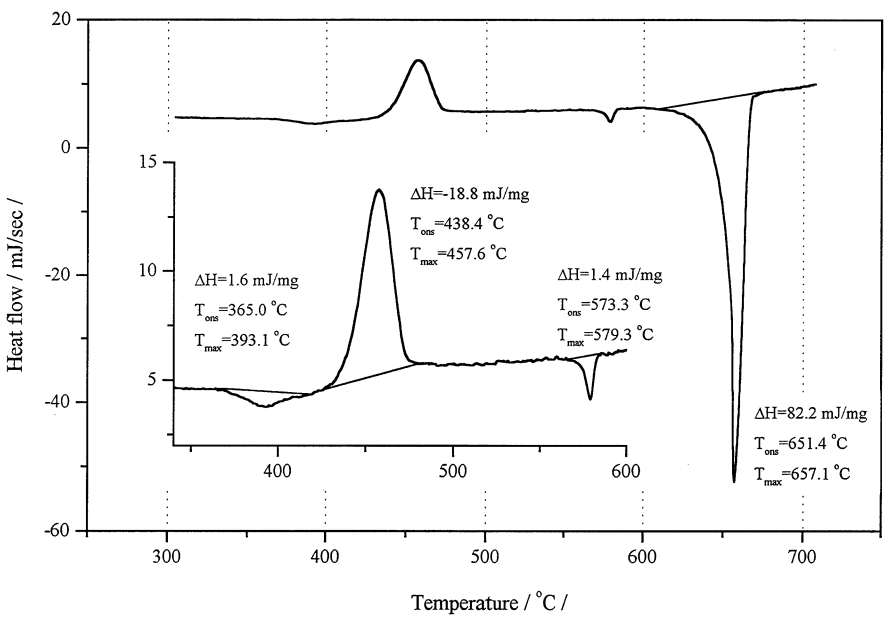


**FIG. 1.** DSC curve of $Bi_2Te_4O_{11}$ sample prepared from a mixture of $Bi_2O_3 + TeO_2$ heated to 720°C for 30 min, then cooled to room temperature by 10°C/min.

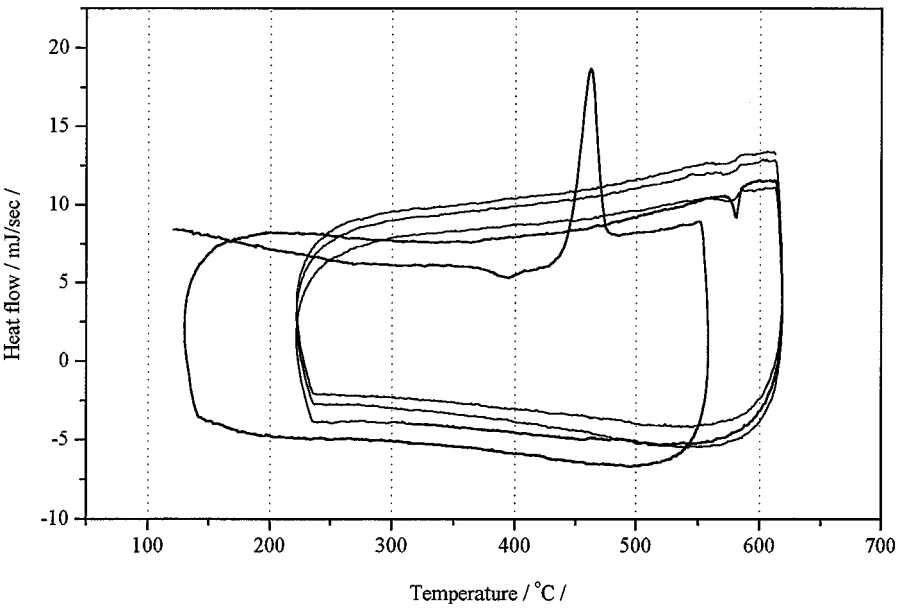


**FIG. 2.** Investigation of the phase transitions by DSC, applying heating and cooling cycles temperature program.

(evenly distributed vacancy), representing a completely disordered chemical structure.

Sample C was identified in our previous work as the monoclinic endproduct of the phase transition. A Rietveld analysis of this phase using the structural model of Rossel and co-workers confirmed its $P2_1/n$ monoclinic structure (2). The small endothermic process observed at 573.3°C in the DSC study raised the question of the existence of an intermediate modification. The Rietveld analysis of sample B using the $P2_1/n$ monoclinic model converged to $R$ values of $R_p = 0.093$, $R_{wp} = 0.126$, $S_{G.o.F.} = 1.74$. These results indicate that both samples B and C have predominantly $P2_1/n$ monoclinic structure. The enlarged portion of Fig. 4 shows that in the case of sample B, partially resolved new satellite reflections superimposed on and in between the $P2_1/n$ reflections are responsible for the poorer fit.

**TABLE 1**
**Structural Data of Cubic $Bi_2Te_4O_{11}$**

| | | | | | |
|---|---|---|---|---|---|
| Formula | | $Bi_2Te_4O_{11}$ | | | |
| Crystal system | | cubic | | | |
| Space group | | *Fm*3*n* (225) | | | |
| *a* (nm) | | 0.56385 (1) | | | |
| | | Atomic positions | | | |
| | *x*/*a* | *y*/*b* | *z*/*c* | $B_{iso}$ | s.o.f. |
| Bi | 0 | 0 | 0 | 3.8(2) | 1/3 |
| Te | 0 | 0 | 0 | 4.6(3) | 2/3 |
| O | 1/4 | 1/4 | 1/4 | 4.8(4) | 11/12 |
| | | Figures of Merit | | | |
| $R_p$ | | 0.078 | | | |
| $R_{wp}$ | | 0.101 | | | |
| $R_{exp}$ | | 0.075 | | | |
| $S_{Goodness\text{-}of\text{-}Fit}$ | | 1.37 | | | |
| Derived $R_B$ | | 0.057 | | | |

The X-ray powder study of samples B and C confirms — in accordance with conclusions of Rossel—that the phase transition of $Bi_2Te_4O_{11}$ from cubic to monoclinic modification is in fact a process of chemical ordering in the cubic [1 1 1] directions. In this process, three cation layers are formed, one favored by tellurium and two by bismuth and tellurium atoms (Bi:Te = 1:1) in a 1–2–1–2 sequence. The basic similarity of samples B and C shows that the thermodynamically favored high–temperature modification is the $P2_1/n$ structure with an oxygen vacancy distribution providing a sequence of rutile-type ($TeO_2$) and fluorite-type ($Bi_2Te_2O_7$) structural slabs. The presence of superlattice satellite reflections in sample B indicates, however, that intermediate or alternative ordering stages may exist either in the cation or in the anion sublattice. To test the existence of a long-range ordering pattern, a site occupancy refinement was attempted in a model using the above positions (including the vacant oxygen sites) but in a degraded $P\bar{1}$ symmetry (a $P1$ model would have been too large for available degrees of freedom). In case of oxygen the refinement oscillated, showing that either the available data set was insensitive to the changes in oxygen vacancy or there was no significantly different long-range oxygen ordering in the sample. When a Bi/Te ratio was refined in each cation position, the $R_p$ dropped from 0.093 to 0.091 with tendencies of Te moving to certain Bi positions. The change, however, was not significant enough to justify postulating a different

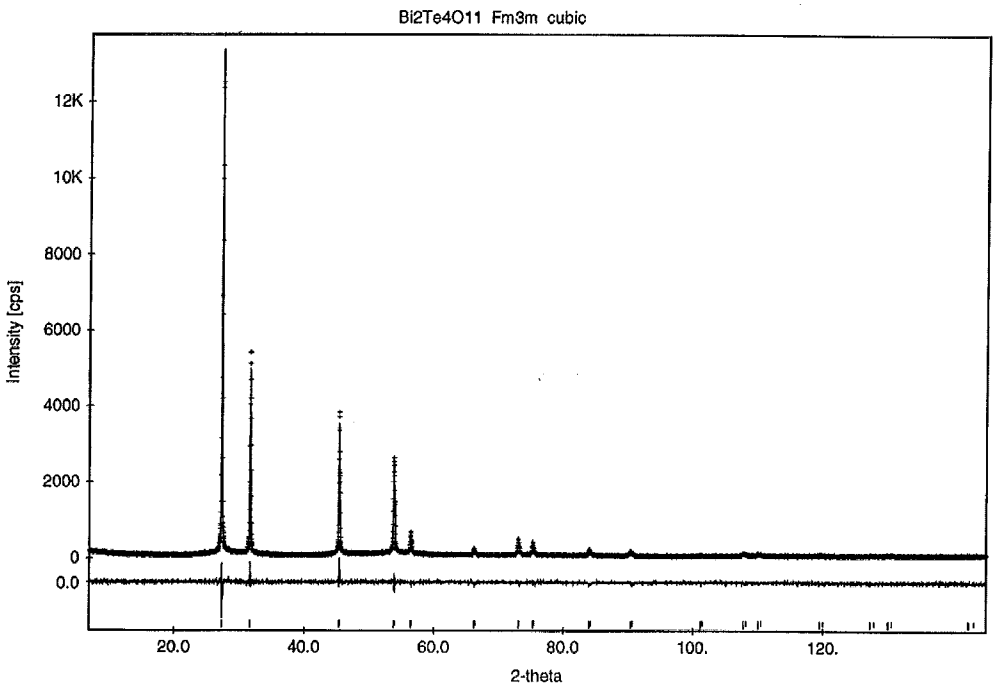


**FIG. 3.** Measured and calculated powder profile of sample A (cubic $Bi_2Te_4O_{11}$) with difference curve and marked theoretical Bragg positions.

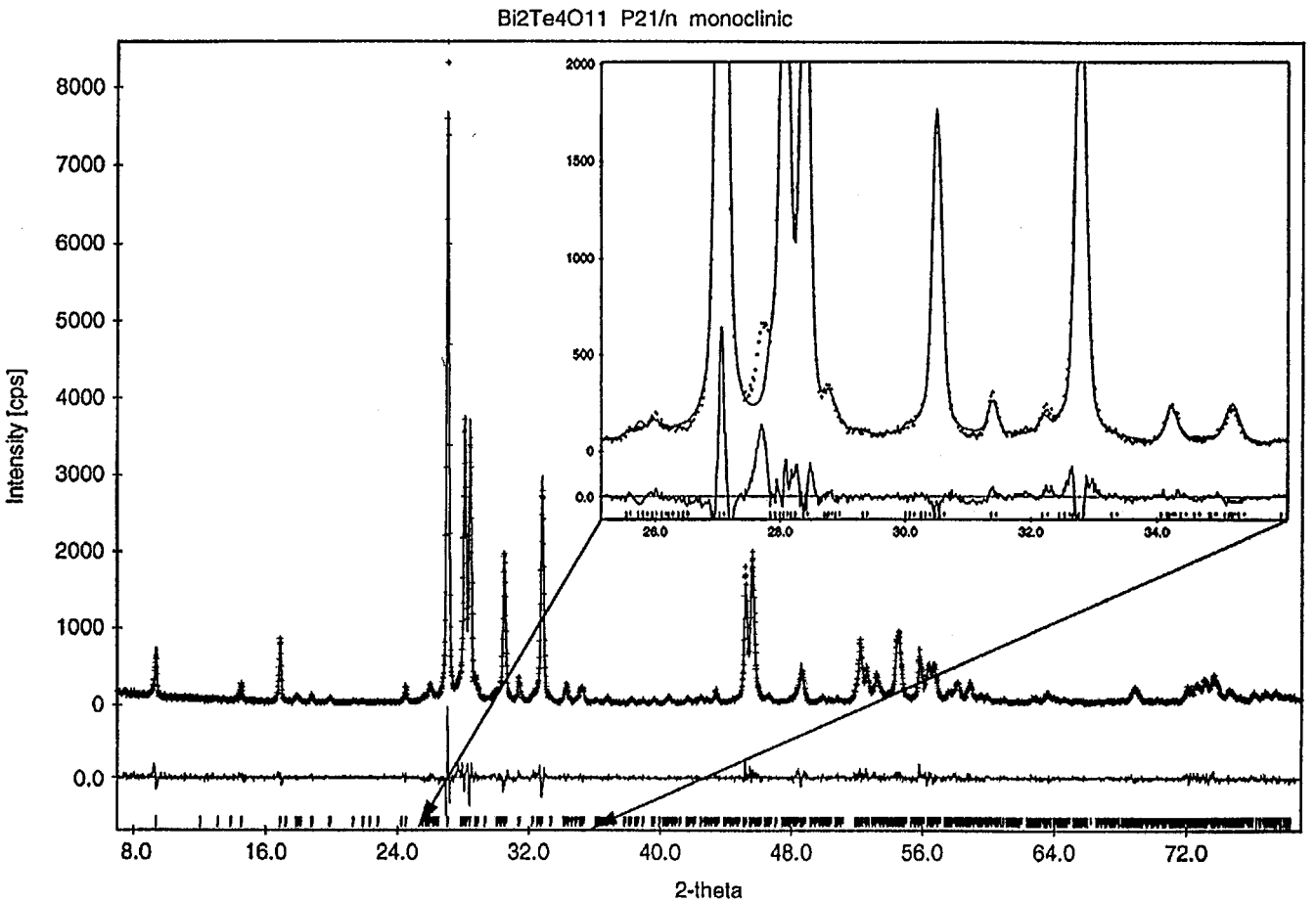


**FIG. 4.** Measured and calculated powder profile of sample B (monoclinic $Bi_2Te_4O_{11}$) showing super-lattice satellite reflections in the enlarged portion.

long-range ordering pattern. The appearance of satellite reflections nevertheless indicates the existence of certain real structural elements in sample B, and the results suggest that they might be attributed to cation ordering, mainly in the $Bi_2Te_2O_7$ layers, rather than an ordering of the oxygen vacancy.

*Electron-Optical Study*

A detailed electron diffraction study to clarify the real structure of this material and to determine the true ordering schemes behind the phase transition from cubic to monoclinic symmetry was undertaken. Figure 5a shows a slightly misoriented [1 $\bar{1}$ 0] projected SAED pattern of crystal from sample A. It reveals that the first process in the transition of the cubic phase is cation ordering along a cubic [1 1 1] direction. The final stage of this ordering is the separation of the metals into the triplets of planes. Every third plane contains only **Te**, and the others are occupied by equal amounts of **Bi** and **Te** with random distribution. The oxygen content is lower than the available anion sites provided by the ideal fluorite structure, and these positions are populated by oxygen in a statistical (random) distribution. The simulated SAED pattern in Fig. 5b is calculated on the basis of the structural model in Fig. 5c. The matching between the observed and simulated patterns is satisfactory.

The next step of transition is the ordering of oxygen vacancy, which was studied in sample B. The SAED patterns proved that the fluorite arrangement of oxygen is relatively stable under the conditions of sample treatment. The oxygen vacancy is concentrated at the Bi-containing layers. Despite great differences between the topology of fluorite–rutile (Figs. 6a, 6b) and solely fluorite-based (Figs. 6c, 6d) structural models, the only characteristic diffraction difference between them is in some weak reflections in their calculated SAED patterns (Fig. 7). Compared to Rossel's model, the fluorite-based structure has extra reflections at

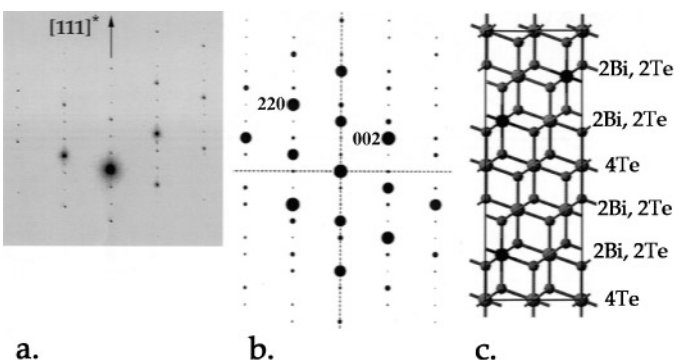


**FIG. 5.** SAED patterns of cubic $Bi_2Te_4O_{11}$. (a) Measured crystal pattern of sample A. (b) Calculated SAED pattern based on assumed structural model. (c) Assumed structural model.

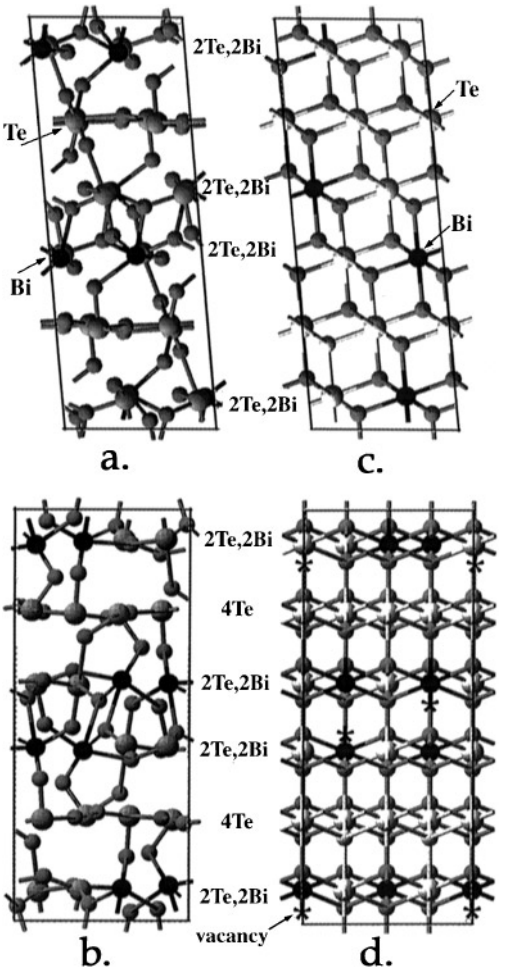


**FIG. 6.** Fluorite-rutile (a, b) and exclusively fluorite-based (c, d) structural models.

places where $l = 2n + 1$ on the 00$l$ row. The experimental [1 0 0] projected SAED pattern of sample B in Fig. 8 corresponds to Fig. 7d and supports the fluorite-based structural model shown in Fig. 6d.

The main part of sample C is $Bi_2Te_4O_{11}$ with $P2_1/n$ symmetry (Fig. 9), but there are several grains in the sample that have traces of ordering characterized by a pure fluorite-type structure shown in Fig. 5. The SAED pattern of Fig. 10 shows the coexistence of the exclusively cation-ordered fluorite-based structure and Rossel's structure. The **c*** of the [0 1 0] projected Rossel's structure ($\mathbf{c}_R^*$, the direction of cation ordering) is near parallel to the $[1\,1\,\bar{1}]_{\text{fluorite}}$, while the structure, as modeled in Fig. 5, is ordered along the [1 1 1] direction of common fluorite sublattice. The boundary between the two phases is irregular. Figure 10 reveals the stability of the fluorite-type arrangement of oxygen atoms. The solid state first-order phase transformation can be assumed at the grain boundaries.

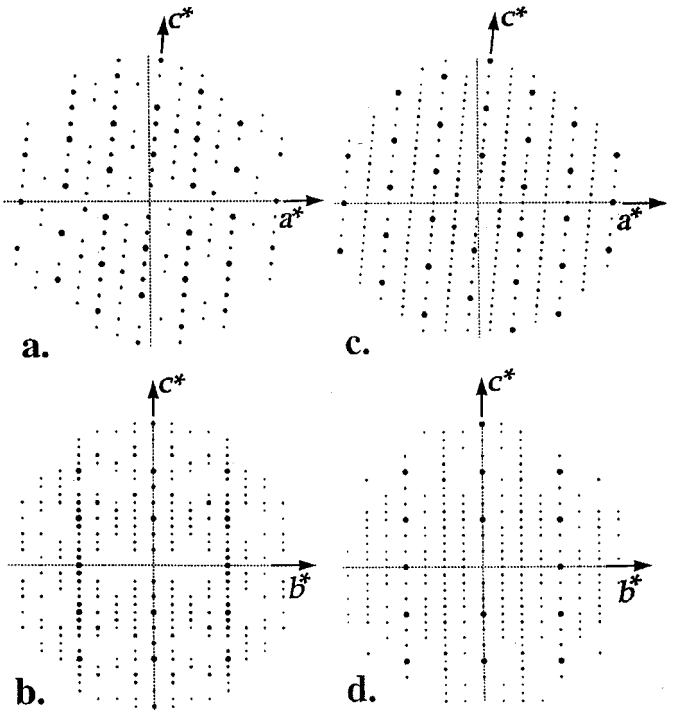


**FIG. 7.** Calculated SAED patterns of Figs. 6a–d.

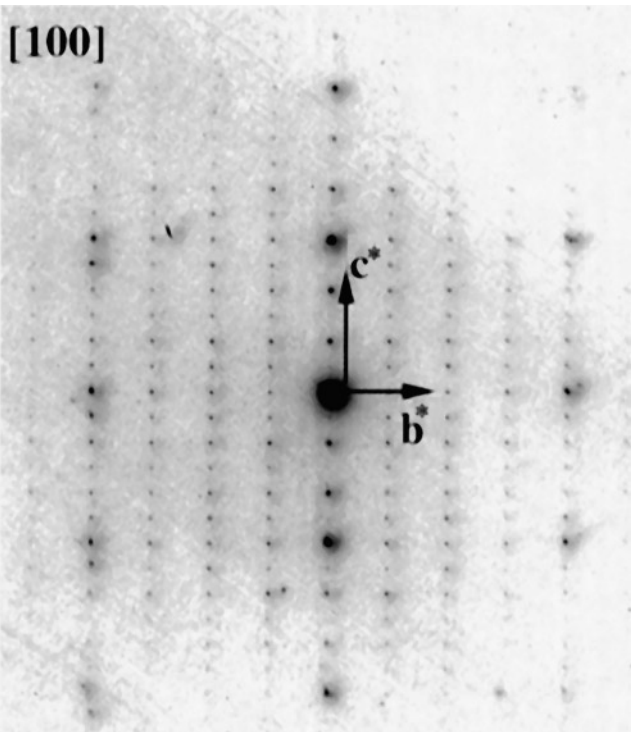


**FIG. 9.** SAED pattern of sample C.

## CONCLUSIONS

Detailed X-ray and electron diffraction studies prove that the metastable cubic phase of $Bi_2Te_4O_{11}$ has *Fm*3*m* fluorite structure. Each cation position is filled with bismuth and tellurium in 1/3–2/3 ratio, while the anion positions are occupied by oxygen in 11/12 site occupancy (evenly distributed vacancy), representing a completely disordered chemical structure.

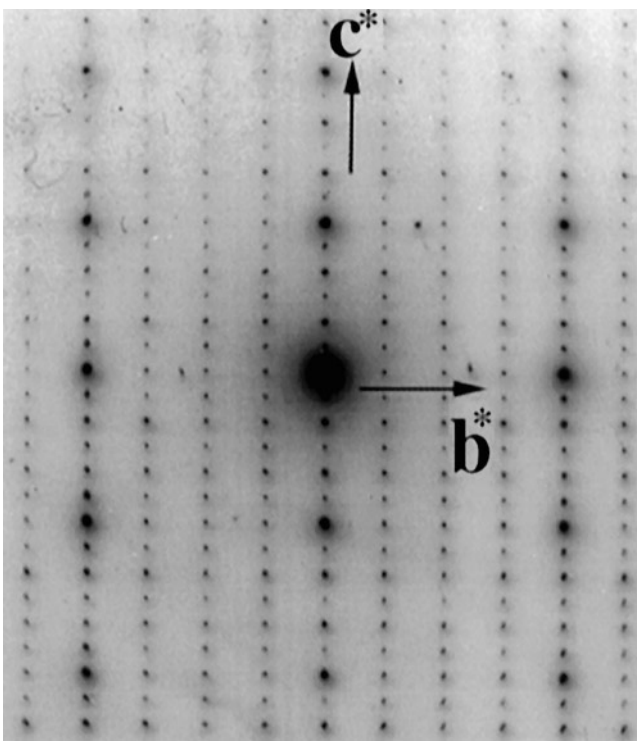


**FIG. 8.** SAED pattern of sample B.

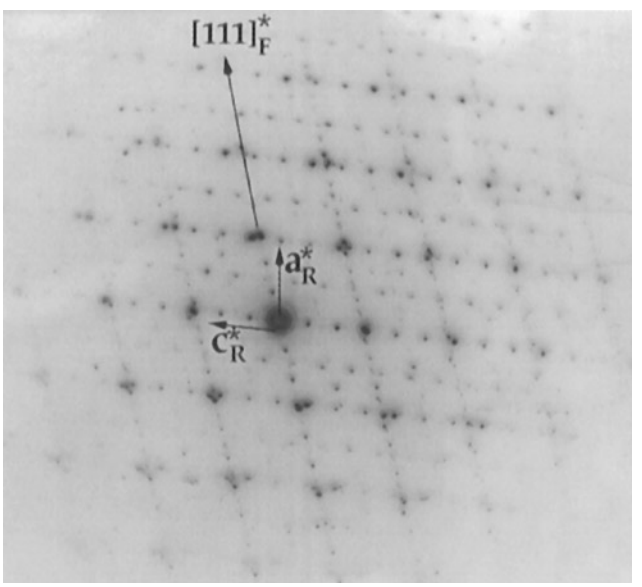


**FIG. 10.** SAED pattern for part of sample C showing the coexistence of the exclusively cation-ordered, fluorite-based structure and Rossel's structure.

The first process in the transition of the cubic phase is the cation ordering along a cubic [1 1 1] direction. The ordering process has a small activation energy, but the structure reordering itself is exotherm. The final stage of this ordering is the separation of the cations into the triplets of planes. Every third plane contains only **Te**, and the others are occupied by equal amounts of **Bi** and **Te** with random distribution. The oxygen content is lower than the available anion sites provided by the ideal fluorite structure, and these positions are populated by oxygen in a statistical (random) distribution.

The next step of transition is the ordering of oxygen vacancy. The SAED patterns prove that the fluorite arrangement of oxygen is relatively stable under the conditions of sample treatment. In most cases the oxygen vacancy is concentrated at the Bi-containing layers and supports the fluorite-based structural model of the $Bi_2Te_2O_7$ structural slabs, while the subsequent $TeO_2$ layer is of rutile-type. The result is monoclinic $Bi_2Te_4O_{11}$ with $P2_1/n$ symmetry. There are, however, several grains in the sample that show the coexistence of the exclusively cation-ordered fluorite-based structure and Rossel's structure. In this case the $TeO_2$ slabs maintain as well the fluorite-type arrangement. The boundary between the two phases is irregular. The solid state first-order phase transformation can be assumed at the grain boundaries.

## REFERENCES

1. Zs. Szaller, L. Pöppl, Gy. A. Lovas, and I. Dódony, *J. of Solid State Chem.* **121,** 251 (1996).
2. H. J. Rossel, M. Leblanc, G. Férey, D. J. M. Bevan, D. J. Simpson, and M. R. Taylor, *Aust. J. Chem.* **45,** 1415 (1992).
3. R. A. Young, A. Sakthivel, T. S. Moss, and C. O. Pavia-Santos, User's Guide to Program, DBWS-9411, School of Physics, Georgia Inst. of Technology, Atlanta, Georgia (1994).
4. H. Marciniak and R. Diduszko, High Pressure Research Center, ul. Sokolowska, 01-142, Warsaw, Poland.